the corresponding theoretical value of 0·961 MHz (calculated as per eqn. 4). The error may be attributed to the higher order effects (specifically, the second pole of the opamps) not accounted for in the analysis in eqns. 1–4. The VCO based on the use of AMs has also been verified using AD534 AMs.

693

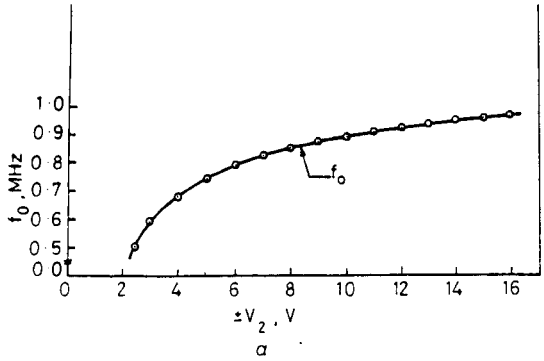

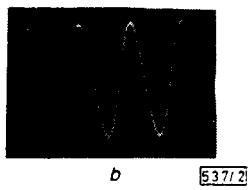

Fig. 2 *Experimental results*

a Variation of oscillation frequency with respect to bias voltage $\pm V_2$ (keeping bias voltage $\pm V_1$ fixed)

b Typical waveform generated by proposed circuit: $f_0 =$ 781·25 kHz; 0·116 V peak to peak

CMOS implementable version: CMOS-compatible versions of the proposed oscillator are possible in conjunction with CMOS opamps, MOS capacitor C_0 and R_0 replaced by either a switched capacitor or a CMOS voltage-controlled linear resistor. One such version has been simulated in SPICE using a CMOS opamp (Fig. 8.3-2 of Reference 2) and a CMOS floating resistor [3] (see Fig. 5.2-5 of Reference 2) in place of R_0. The simulations have shown results which are almost similar to those described in the preceding Section.

Conclusions: An extremely simple sinewave oscillator configuration is introduced which uses the opamp compensation poles in the design and employs only two external passive components (a resistor and a grounded capacitor). The proposed circuit can generate sinusoidal oscillations up to a frequency nearly equal to the geometric mean of the GBP of the two opamps used. With some modifications, using an additional opamp or analogue multipliers, the oscillations can be made voltage-controllable. Using a CMOS opamp, MOS capacitor and a CMOS floating resistor, a CMOS-compatible version of the proposed oscillator is also possible. In such a case, the use of a single grounded capacitor is an advantage as the bottom plate parasitic capacitance is eliminated altogether and the top plate parasitic capacitance can be accounted for easily as it becomes parallel to the main capacitance.

5th January 1993

R. Senani (*Linear Integrated Circuits Lab., Department of Electronics and Communication Engineering, Delhi Institute of Technology, Old I.G. Block, Kashmere Gate, Delhi 110006, India*)

References

1 SENANI, R.: 'Network transformations for incorporating nonideal stimulated immittances in the design of active filters and oscillators', *IEE Proc. G*, 1987, **134**, (4), pp. 158–166

2 ALLEN, P. E., and HOLBERG, D. R.: 'CMOS analog circuit design' (Holt, Reinhart and Wilson, Inc., 1987), Chap. 5, pp. 211–218 and Cahp. 8, pp. 436–445

3 BANU, M., and TSIVIDIS, Y.: 'Floating voltage-controlled resistors in CMOS technology', *Electron. Lett.*, 1982, **18**, (15), pp. 678–679

100% REFLECTIVITY BRAGG REFLECTORS PRODUCED IN OPTICAL FIBRES BY SINGLE EXCIMER LASER PULSES

J.-L. Archambault, L. Reekie and P. St. J. Russell

Indexing terms: Optical fibres, Excimer lasers

It is shown for the first time that fibre gratings with reflectivities in excess of 99·8% and fractional bandwidths of 0·005 (7·5 nm or 970 GHz at 1550 nm) can be written by interferometric side exposure of a fibre core to a *single* 40 mJ UV pulse of 20 ns duration at 248 nm. These highly efficient reflectors are formed by a new mechanism in which the core glass fuses, resulting in a very large periodic modulation of the refractive index. They are stable at temperatures as high as 800°C.

Introduction: The holographic technique developed by Meltz and co-workers, where the photosensitive core of an optical fibre is exposed to two interfering UV beams [1], has now been widely adopted as the most effective way of producing fibre gratings, because it requires very little fibre preparation, leaves the fibre intact and yields very low loss gratings. Recently, the use of high pulse energy, line-narrowed, KrF excimer lasers has made it possible to reduce the writing time to 20 ns, the duration of a single pulse [2]. We recently demonstrated that high reflectivity fibre gratings could be written in this way [3]. Here we report the results of further experiments aimed at improving the performance of the single-pulse gratings and investigating the nature of the index-changing mechanisms at high UV intensities.

Experiment: The interferometer used for grating writing is the same as previously described [3]. The Lambda Physik EMG-150 excimer laser fires 0·1 J, 20 ns pulses at 248 nm, with a coherence length of 25 mm. Its pulse energy was controlled using a half-wave plate and polariser arrangement and monitored accurately with a pyroelectric energy meter, part of the beam being tapped off at a fused silica optical flat. The interferometer was set up to produce fibre gratings with a centre wavelength near 1550 nm. The UV beam was partially focused onto the fibre through a pair of cylindrical lenses, resulting in a beam cross-section of approximately $15 \times 0{\cdot}3\,mm^2$ at the fibre, the long dimension being parallel to the fibre axis. The fibre used had a germania-doped (15 mol%) core with a numerical aperture of 0·25.

A series of single-pulse gratings were produced to explore the relationship between pulse energy and grating strength. In each case, a short section of fibre was stripped of its coating, a single pulse was fired and the resulting grating was characterised by sending the output of a broadband LED into the fibre through a 3 dB coupler and measuring the reflected or transmitted light in an optical spectrum analyser. In total, 36 gratings were written over a period of 4 h. The 0·3 mm beam width ensured that sample-to-sample variations in positioning the fibre did not significantly affect the amount of UV energy hitting the core. The interferometer was aligned once at the very beginning of the experiment and no further adjustments were made, apart from rotating the half-wave plate. Afterwards, several gratings were placed inside a furnace and tested for thermal stability at temperatures ranging from 700 to 1000°C for 24 h periods.

Results and discussion: The index modulation (peak-to-peak) of each grating was estimated from its reflection spectrum using the results of standard coupled-mode theory. All these data are assembled in Fig. 1, where it is immediately apparent that a sharp threshold occurs at a pulse energy of ~30 mJ; when the pulse energy is increased from 20 to 40 mJ, the photoinduced index modulation goes up by more than two orders of magnitude. Below this threshold (from 10 to 25 mJ), the index modulation seems to grow linearly with pulse energy, whereas above it (40 to 60 mJ) the index modulation appears to saturate. A striking feature of Fig. 1 is that the index changes can be very high, as much as 0·006, which is comparable to the core-cladding index difference (0·02). For conve-

nience we label gratings formed in the low and high index regimes type I and type II, respectively. Type II gratings have very high reflectivities and large bandwidths (see Fig. 2). The transmission spectrum showed at least 26 dB (limited by measurement system) extinction at the Bragg wavelength, which means that only 0·2% of the light is transmitted. The calibrated reflection spectrum confirms that this single-pulse grating is nearly 100% reflecting. The irregularities in the spectra are a sign of grating non-uniformity, which is not surprising because the non-uniformities in the excimer beam profile will be strongly magnified by the highly nonlinear response mechanism of the core glass. Type II gratings pass wavelengths longer than the Bragg wavelength, whereas shorter wavelengths are strongly coupled into the cladding, as is observed for etched or relief fibre gratings [4]. When all-lines of an argon-ion laser were launched in the core, most of the light could be seen diffracting out of one side of the fibre, each laser line being well separated in angle. This indicates that the index modulation is not uniform across the core, permitting the grating to operate as an effective wavelength selective tap.

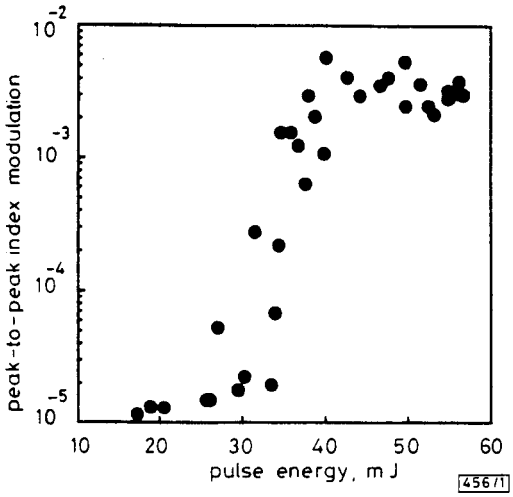

Fig. 1 *Peak-to-peak modulation of refractive index for different pulse energies*

Notice the sharp threshold at around 35 mJ, and the fact that doubling the pulse energy from 20 to 40 mJ produces a ×100 increase in index modulation

The results of stability tests of the type II gratings at elevated temperatures are summarised in Fig. 3. Below 800°C and for periods of ~24 h, no significant changes were observed in the grating reflectivities. At 900°C, the grating under test decayed quite slowly and a permanent (or perhaps very slowly decaying) component appeared. At 1000°C, most of the grating had disappeared after 4 h. Type I gratings written with pulse energies below the 30 mJ threshold were erased within seconds at 450°C. These results provide evidence that the mechanism behind high reflectivity type II single-pulse gratings differs from the usual type I mechanism.

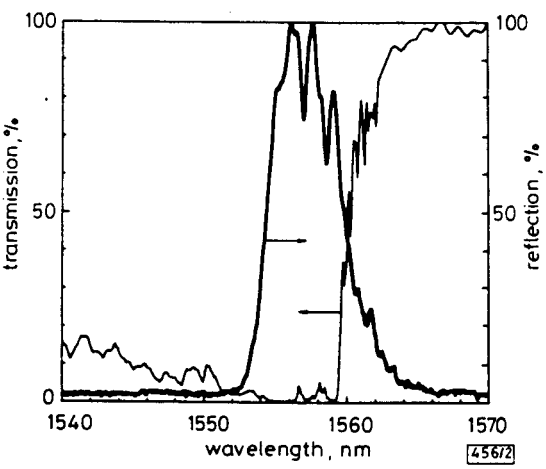

Fig. 2 *Reflection and transmission spectra of typical type II grating*

For wavelengths below the Bragg wavelength (1556 nm) light is coupled strongly into the cladding

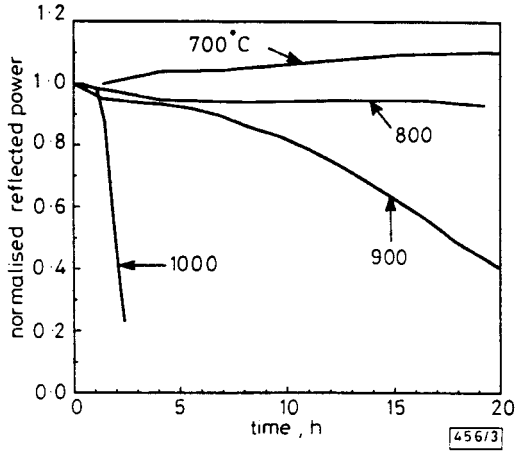

Fig. 3 *Temperature stability of type II gratings*

The response curve in Fig. 1 suggests that there is a critical level of absorbed energy which triggers off some highly nonlinear mechanism, provoking dramatic changes in the glass. On examining a 40 mJ type II grating in an optical microscope, a damage track was seen at the core-cladding interface (see Fig. 4). This damage region appears only in type II fibre gratings, which suggests that it may be responsible for the large index change. The fact that it is localised on one side of the core suggests also that most of the UV light has been absorbed or scattered there, perhaps never reaching the other side. Similar damage tracks are visible in the gratings formed in the Ge–B codoped fibre used in our earlier experiments [3]. In that case, however, the threshold occurred at higher fluences, probably because of a lower absorption at 248 nm.

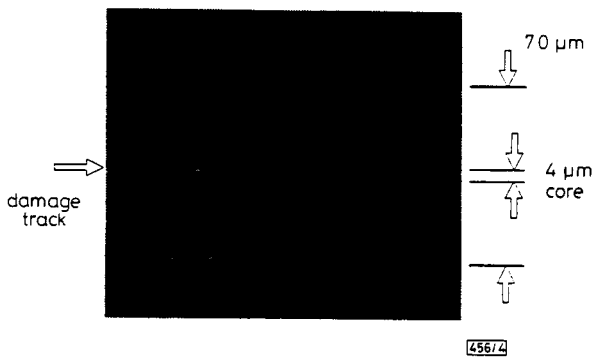

Fig. 4 *Photograph (× 1000) of core after inscription of type II grating*

The core is the light coloured region in the centre (4 μm wide) and the damage track of intermittent dark pits is visible on its upper edge

The damaged region is reminiscent of the damage track left behind after passage of the fibre fuse, where thermal breakdown in the fibre core causes a travelling hot spot at several thousand degrees Celsius, fuelled by absorption of the guided laser light [5, 6]. From recent measurements [7] we estimate the absorption in our fibre core to be 0·3 dB/μm at 248 nm. Under our experimental conditions, it may be shown that a 40 mJ UV pulse will cause an instantaneous temperature rise of several thousand degrees Celcius. At such temperatures the absorption will rise dramatically, explaining the sharp onset of type II grating formation.

Conclusions: In conclusion, a new regime of side-written grating formation has been discovered, permitting reflectivities in excess of 99·8% and fractional bandwidths of 0·005 to be achieved by exposure to a single 20 ns pulse at 248 nm. These type II gratings form above a sharp threshold in pulse energy and are much more stable than type I gratings, surviving 24 h without degradation at 800°C. The superior temperature

handling properties of type II gratings will make them useful in fibre systems operating in hostile environments.

7th January 1993

J.-L. Archambault, L. Reekie and P. St. J. Russell (*Optoelectronics Research Centre, University of Southampton, Southampton SO9 5NH, United Kingdom*)

References

1 MELTZ, G., MOREY, W., and GLENN, W. H.: 'Formation of Bragg gratings in optical fibres by a transverse holographic method', *Opt. Lett.*, 1989, **14**, pp. 823–825

2 ASKINS, C. G., TSAI, T. E., WILLIAMS, G. M., PUTNAM, M. A., BASHKANSKY, M., and FRIEBELE, E. J.: 'Fibre Bragg reflectors prepared by a single excimer pulse', *Opt. Lett.*, 1992, **17**, pp. 833–835

3 ARCHAMBAULT, J.-L., REEKIE, L., and RUSSELL, P. ST. J.: 'High reflectivity and narrow bandwidth fibre gratings written by single excimer pulse', *Electron. Lett.*, 1993, **29**, (1), pp. 28–29

4 RUSSELL, P. ST. J., and ULRICH, R.: 'The grating fiber-coupler as a high resolution spectrometer', *Opt. Lett.*, 1985, **10**, pp. 291–293

5 HAND, D. P., and RUSSELL, P. ST. J.: 'Solitary thermal shock waves and optical damage in optical fibres', *Opt. Lett.*, 1988, **13**, pp. 767–769

6 KASHYAP, R., and BLOW, K.: 'Observation of catastrophic self-propelled self-focusing in optical fibres', *Electron. Lett.*, 1988, **24**, pp. 47–48

7 WILLIAMS, D. L., AINSLIE, B. J., KASHYAP, R., CAMPBELL, R., and ARMITAGE, J. R.: 'Broad bandwidth highly reflecting gratings formed in photosensitive boron codoped fibres'. Proc. European Conf. on Optical Communication, ECOC '92, 1992, pp. 923–926

OPTIMUM CORE DESIGN FOR ERBIUM-DOPED INTEGRATED OPTICAL AMPLIFIERS IN SILICA-ON-SILICON

T. Rasmussen, O. Lumholt, J. H. Povlsen and A. Bjarklev

Indexing terms: Integrated optics, Optical amplifiers, Optical waveguides, Lasers

The gain an Er/P-doped integrated optical waveguide amplifier has been calculated as a function of waveguide core design, pump power, and background loss. The optimum core width varies from 2 to 3 μm for pump powers close to the threshold for amplification up to 3–5 μm for high gain operation.

Introduction: Over the last two years several laboratories have presented results on optical amplification in rare earth-doped integrated optical waveguide amplifiers. For telecommunication purposes, Er/P-doped silica-on-silicon components are especially interesting due to their low loss coupling to optical singlemode fibres and amplification around 1·55 μm coinciding with the lower loss minimum in silica fibres. Relatively high gains (10 dB) have been obtained for modest pump powers (145 mW) [1]. We present the results of a rigorous analysis of the gain in Er-doped, step refractive index silica waveguides. When we optimise the amplifier for maximum gain a quadratic core cross-section of the waveguide is considered as this results in a circular symmetric fundamental mode that the fundamental mode of optical fibres. We show how the optimum waveguide design (core width and waveguide length) depends on the pump power level and the background loss.

Model: The basic amplifier model is described in detail in Reference 2. This model is developed only for the description of light propagation in optical fibres, and excellent results have been obtained in comparison with measurements on these [3]. Minor modifications are consequently requested for the description of waveguides with a rectangular core cross-section. The mode profiles of the fundamental E^x_{11} or E^x_{11} mode [4], have replaced the LP_{01} description. Also, the waveguide background loss, which in integrated optics is several decades larger than in the fibres, is now included. Emission and absorption cross-sections (see the inset of Fig. 1) are

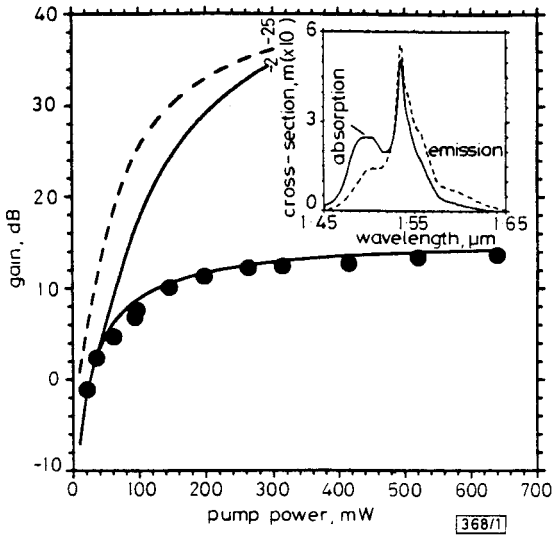

Fig. 1 *Gain as function of pump power*
- ● measured data read from Reference 1
- ——— (lower) our calculations for this amplifier
- ——— (upper) calculated with optimised length
- - - - calculated with optimised length and core size

Inset: absorption and emission cross-section spectra for Er^{3+} in P-doped silica

sampled from presented fluorescence and absorption measurements on Er/P-doped integrated waveguides [1]. Their absolute values are determined as in Reference 5 by considering a 13·7 ms lifetime of the upper laser level [6] and a refractive index difference of 1·2% [1]. These values correspond to waveguides with an 8 wt% P-doped core. The data used for the calculations are listed in Table 1. The pump wavelength is 0·98 μm and the signal wavelength is 1·535 μm. The latter corresponds to the peak in the emission cross-section. We assume that the amplifier is pumped from the same end at which the signal enters the waveguide. As the lowest reported background loss for P-doped silica-on-silicon channel waveguides is $\sim\alpha = 0{\cdot}03$ dB/cm [7], we performed calculations with the background loss equal to this value. We also calculated the optimum core design with more realistic loss values for Er/P-doped planar waveguides of 0·1 and 0·15 dB/cm [1].

Table 1 PARAMETERS USED IN CALCULATIONS

Pump wavelength (λ_p)	0·980 μm
Signal wavelength (λ_s)	1·535 μm
Er concentration	0·55 wt%
Spontaneous emission lifetime	13·7 ms
Absorption cross-section at λ_p	$2{\cdot}2 \times 10^{24}$ m²
Absorption cross-section at λ_s	$5{\cdot}1 \times 10^{25}$ m²
Emission cross-section at λ_s	$5{\cdot}6 \times 10^{25}$ m²
Refractive index difference	1·2%
Signal input power	0·1 μW

Results: Fig. 1 presents amplifier gains as a function of pump power calculated for an amplifier identical to one that was experimentally examined [1]. The lower solid line is calculated for a fixed core cross-section of $8 \times 7\,\mu$m² and a waveguide length of 19·4 cm, identical to the experimentally investigated amplifier. The background loss is 0·1 dB/cm and all the other amplifier data are as listed in Table 1. The measured gain, read from Reference 1, is shown by the circles. As can be seen the calculated gain as function of pump power matches the measured values very well. As the length of 19·4 cm is only optimum for a pump power of 33 mW, a series of calculations has been made to determine the length giving the maximum gain for each considered pump power level. The maximum gain for a fixed core cross-section of $8 \times 7\,\mu$m² and with optimised length as described above is shown as the